

Modeling of noise due to distant seismic exploration in the Marginal Ice Zone

Dag Tollefsen and Elin M. Dombestein

Norwegian Defence Research Est. (FFI), Maritime systems division, 3191 Horten, Norway.

Hanne Sagen

Nansen Environmental and Remote Sensing Center (NERSC), 5006 Bergen, Norway.

Summary

Ambient noise recorded on sonobuoys deployed in the Marginal Ice Zone (MIZ) of the Fram Strait in June of 2011 contained high levels of low-frequency (10–200 Hz) noise attributed to distant seismic exploration. A reduction of noise levels with distance into the MIZ was observed and explained in terms of attenuation due to the ice cover. In this paper, transmission loss in the ice-ocean environment of the MIZ is modeled using a raytrace numerical model that includes reflection loss due to a range-dependent elastic ice cover. Environmental model input is taken from the TOPAZ4 ocean data assimilation system and from a satellite image, with a two-zone ice model developed. Transmission loss predictions explain the observed noise level reductions.

PACS no. 43.30.Nb, 43.30.Ma

1. Introduction

Long-term noise recordings in Arctic waters have reported seasonal occurrence of low-frequency noise due to distant seismic exploration [1,2]. Airgun signals were recorded at long range in ice-free and partially ice-covered Arctic waters, with measured transmission loss fitted by geometric spreading laws [3]. Short-term synoptic recordings of ambient noise at twenty-two locations in the Marginal Ice Zone (MIZ) of the Fram Strait were collected in June 2011. Data analysis showed high noise levels at low frequencies (10–200 Hz) which was attributed to distant seismic exploration, and a reduction of noise levels with distance into the MIZ was observed [4]. The MIZ comprises highly variable ice conditions ranging from open water to ice-covered regions composed by a mixture of new frozen, first year ice and multi-year ice. Below ice-covered regions an oceanographic layer with cold and less saline water causes ducting of acoustic energy; this layer diminishes in thickness across the MIZ and disappears in the open ocean. The effect of ice/ocean conditions in this variable environment on noise due to distant seismic exploration appears to have been less studied. This paper develops a range-dependent sea-ice model for the MIZ of the Fram Strait, presents

results from modeling of transmission loss, and compares loss predictions with observed noise level reductions.

2. Noise measurements

Sonobuoys were deployed by P-3C aircraft on June 9, 2011 over an area of the Fram Strait bounded by 78° to 79° 30' N and 3° W to 3° E. The experiment area (Fig. 1) covered the MIZ from open water to compact ice, and was close to an area of similar measurements in April of 1987. Hydrophone acoustic data (sensor depth 400 ft.) considered here was recorded over a 1 hr time period starting at 10:54Z. Inspection of spectrograms (not shown) revealed distinct time arrivals of low-frequency energy attributed to seismic exploration. Data were processed in 1/3-octave frequency bands; spectrum estimation used ten consecutive 3 s samples of data, with median noise spectral density levels (NSL) in dB re 1 $\mu\text{Pa}^2/\text{Hz}$ estimated for each buoy. Figure 1 shows the NSL at 100 Hz for all buoys. The highest levels (86–88 dB) are observed at buoys in the open ocean; noise levels decrease with distance into the ice cover with lowest levels (79–80 dB) at buoys within compact ice. The levels exceeded those measured in 1987 by up to 12 dB, despite low sea state conditions [4].

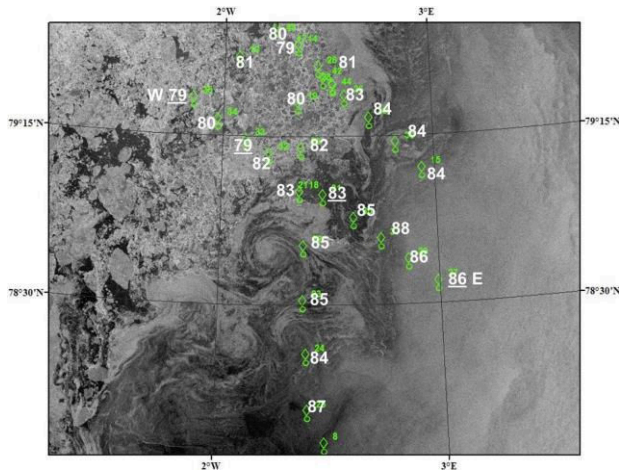


Figure 1. Map of the Fram Strait experiment area. Symbols (green) indicate sonobuoy locations. Numbers (white) indicate median noise spectral density levels (dB re $1\mu\text{Pa}^2/\text{Hz}$) at 100 Hz. The background is a RadarSat© image date 2011/6/9 10:14Z.

Figure 2 shows median NSL (in dB re $1\mu\text{Pa}^2/\text{Hz}$) for buoys along the line from E (open water) to W (compact ice) for 1/3-octave frequency bands of 31, 50, 100 and 200 Hz; the horizontal axis is range from buoy E. At 31 Hz the NSL varies by 5 dB between the buoys but with no apparent reduction with range. At higher frequencies, the NSL decreases by 1 to 9 dB from open water to compact ice. For example, the decrease is 2 dB at 50 Hz, 7 dB at 100 Hz, and 9 dB at 200 Hz.

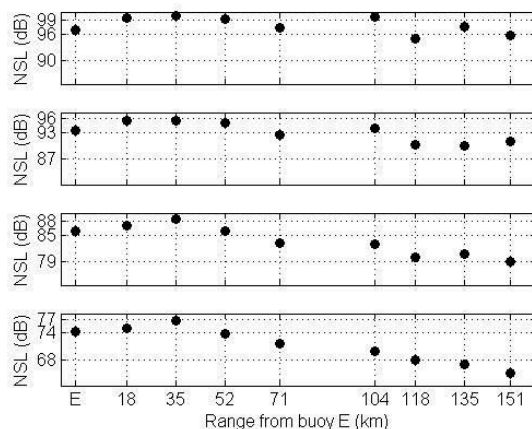


Figure 2. Median noise spectral density level (dB re $1\mu\text{Pa}^2/\text{Hz}$) at 31 (upper panel), 50, 100 and 200 Hz (lower panel) for nine buoys along E to W. Horizontal axis is range from buoy E.

3. Modeling of transmission loss

Transmission loss from the location of a distant seismic survey is modeled by use of the range-dependent raytrace model BELLHOP [5], with an environment model described in this section.

Ongoing seismic surveys on the day of the experiment were at ranges in excess of 1400 km southeast of the experiment area [4].

3.1. Water-column and seabed properties

Environmental input was taken from the TOPAZ4 coupled ocean–sea ice model [6], with temperature and salinity versus depth forecast profiles extracted along transects from the source position to each buoy. The profiles were converted to sound speed versus depth using the McKenzie formula and interpolated in range using the quadrilateral interpolation scheme in BELLHOP. Figure 3(a) shows an interpolated sound speed section from the Norwegian Shelf (left) to the Fram Strait (right). Figure 3(b) shows selected profiles at ranges of 630, 930 and 1520 km. Propagation from the Shelf is dominated by the deep sound channel until approximately 800 km range, where colder Polar Water forms upward-refracting profiles with a weak surface sound channel. Propagation effects through this front were studied in [7].

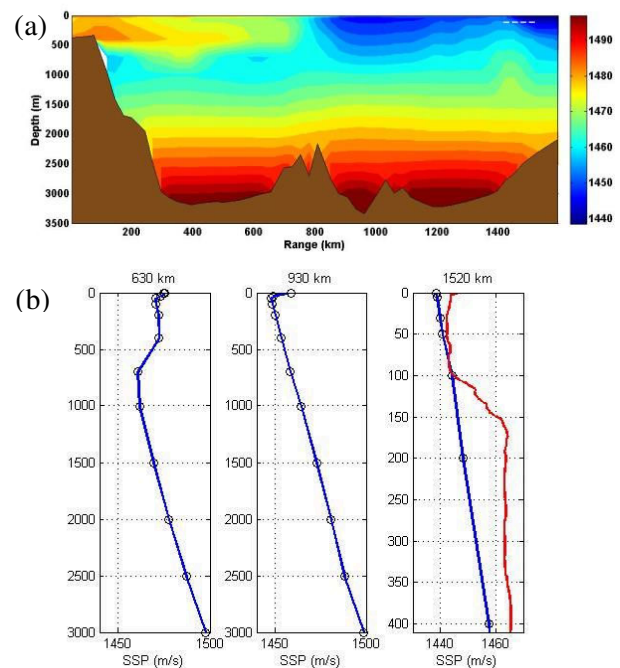


Figure 3. (a) Sound speed (m/s) section based on TOPAZ4 model profiles from the Norwegian Shelf (left) to the Fram Strait (right). (b) Selected model speed profiles (blue) and a measured profile (red).

The rightmost model profile in Fig. 3(b) is within compact ice. For comparison is shown a measured profile in compact ice in September of 2010 [8]; this (red curve) shows a distinct surface duct not seen in the model profile. For attenuation of sound in seawater, an approximation to Leroy's

equation was used. Bathymetry profiles were taken from TOPAZ4. Seabed geoacoustic parameter values were set to compressional wave speed $c=1520$ m/s, density $\rho=1.5$ g/cm³, attenuation $\alpha=0.1$ dB/ λ (wavelength λ).

3.2. Sea-ice zones and thickness

The RadarSat(c) image was visually inspected for boundaries between open water/diffuse ice and diffuse ice/compact ice. Figure 4 shows these two boundaries, and the predicted ice thickness from the TOPAZ4 model. The compact ice edge (red) compares well with the TOPAZ4 predicted ice edge, while the diffuse ice edge (blue) is not predicted. Based on the identified ice edges, a three-zone environment consisting of open water, diffuse ice, and compact ice was used in the following.

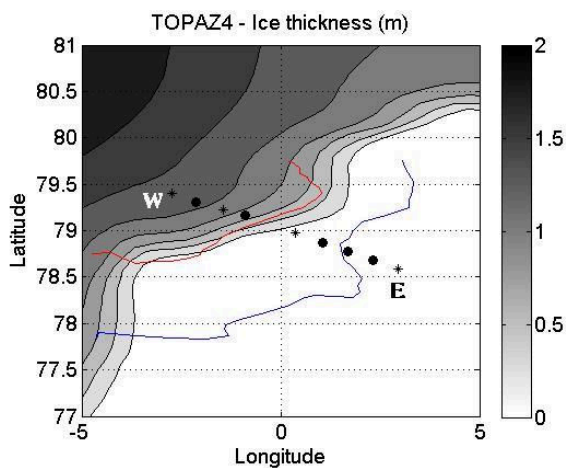


Figure 4. Ice thickness (m) from the TOPAZ4 model, and location of diffuse ice edge (blue) and compact ice edge (red) as interpreted from the RadarSat image. Symbols indicate the positions of buoys along the E-W line; stars indicate the four positions used in modeling.

Measurements of ice thickness in the Fram Strait in September of 2010 yielded a mean value of 1.3 m with a standard deviation of 0.6 m [9]. We assumed mean ice thickness of 1.2 m in the diffuse ice region, and 1.8 m in the compact ice region.

3.3. Sea-ice properties

Measurements of sea-ice acoustic properties are available in the literature; few of these are from the MIZ. The parameters used in the following [10] are based on analysis of seismic-wave signals recorded on ice-mounted geophones on a 2-m thick ice floe (predominantly first year ice) in the central Arctic. The values are $c=2900$ m/s and $\alpha=2.6$ dB/ λ , with shear speed 1670 m/s and attenuation 1.6 dB/ λ , in good agreement with

previous data from the Arctic. For sea-ice density we used $\rho=0.91$ g/cm³. Rough sea-ice and ice-air boundaries are modeled by Gaussian roughness spectra with standard deviation $\sigma_b=0.6h$ at the sea-ice boundary (mean thickness h) and $\sigma_i=0.25\sigma_b$ at the air-ice boundary (correlation length 40 m) [11]. The complex reflection coefficient versus grazing angle for a sea-ice-air model with rough interfaces was computed with the OASES model [5]. Figure 5 shows the reflection coefficient for models with ice thickness of 1.2 m (black) and 1.8 m (red), respectively, at three frequencies; reflection loss increases with ice thickness (and frequency) for this model.

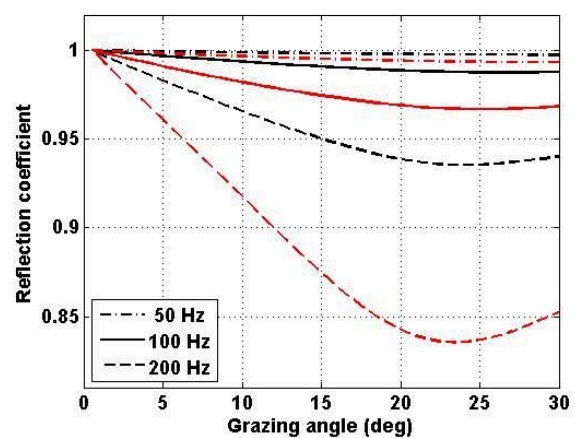


Figure 5. Reflection coefficient versus grazing angle for layered sea-ice-air model with 1.2 m (black) and 1.8 m (red) ice thickness, at three frequencies. Model parameters are defined in the text.

4. Results

The BELLHOP model was run with environment models that included (a) no ice cover, (b) a constant 1.2-m thick ice cover from the diffuse ice edge, (c) a two-zone ice cover (thickness 1.2/1.8 m) defined in section 3.2, and (d) a two-zone ice cover with the measured sound speed profile of Fig. 3(b) applied within the compact ice zone. A point source at depth 12 m was used.

Figure 6 shows modeled transmission loss over the extent of the ice zones to buoy W at 200 Hz for models (a)–(d). Lowest loss is observed for model (a), highest loss is observed for model (d). Models (b) and (c) are identical to the compact ice edge (range 1470 km); an additional 2–3 dB loss in compact ice is observed for model (c) due to increased ice reflection loss from a thicker ice cover. Further 1–2 dB loss related to effects of the surface duct can be observed for model (d).

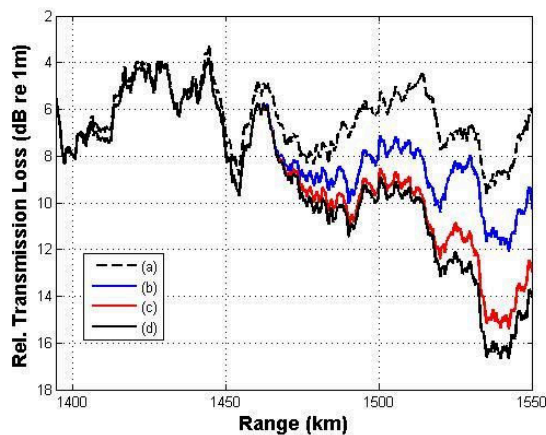


Figure 6. Modeled transmission loss at 200 Hz (relative to loss at the ice edge) versus range for environment models with no ice cover (dashed) and three models with ice cover (see text for details).

Figure 7 compares modeled transmission loss with observed reduction in noise levels at three buoys marked by stars in Fig. 4. Loss predictions, relative to buoy E, are for environmental models with no ice (open circles) and the two-zone ice cover model (d) (triangles). The loss predictions for model (d) are within 3 dB of the observed noise level reductions for all buoys and frequencies.

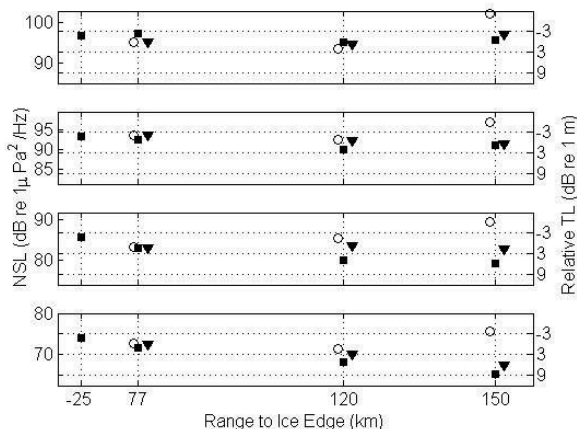


Figure 7. Measured noise levels and modeled transmission loss in the Fram Strait Marginal Ice Zone at frequencies 31 Hz (upper), 50 Hz, 100 Hz, and 200 Hz (lower panel). Measurements (squares) are median noise spectral density levels in dB re $1 \mu\text{Pa}^2/\text{Hz}$ (left axis) from sonobuoys in open water (left), diffuse ice, and compact ice (right), range to the diffuse ice edge on horizontal axis. Transmission loss in dB re 1 m (right axis) is relative to buoy E in open water, for environmental models with a two-zone ice cover (triangles) and no ice cover (open circles).

5. Summary

High noise levels were measured at low frequencies in the MIZ of the Fram Strait and attributed to distant seismic exploration. The 1–9 dB reductions in noise levels (50–200 Hz) observed over ~150 km range from open water to compact ice were explained to within 3 dB by numerical modeling of transmission loss. The model included reflection loss due to a rough elastic ice cover in two ice zones of the MIZ. The ice zone model is subject to refinement as more data on ice distribution is analyzed.

Acknowledgement

Fieldwork supported by the Royal Norwegian Air Force. Work at NERSC supported by The Research Council of Norway under the WIFAR and UNDER-ICE programs.

References

- [1] Moore, S. M., Stafford, K. M., Melling, H., Berchok, C., Wiig, Ø., Kovacs, K. M., Lydersen, C., Richter-Menge, J. (2012). "Comparing marine mammal acoustic habitats in Atlantic and Pacific sectors of the High Arctic: year-long records from Fram Strait and the Chukchi Plateau," *Polar Biol.* **35**, 475–480.
- [2] Klinck, H., Nieukirk, S. L., Mellinger, D. K., Klinck, K., Matsumoto, H., and Dziak, R. P. (2012). "Seasonal presence of cetaceans and ambient noise levels in polar waters of the North Atlantic," *J. Acoust. Soc. Am.* **132**, EL176–EL181.
- [3] Thode, A., Kim, K. H., Greene, C. R., and Roth E. (2010). "Long range transmission loss of broadband seismic pulses in the Arctic under ice-free conditions," *J. Acoust. Soc. Am.* **128**, EL181–EL187.
- [4] Tollefsen, D. and Sagen, H. (2014). "Seismic exploration noise reduction in the Marginal Ice Zone," *J. Acoust. Soc. Am.* **136**, EL47–EL52.
- [5] Acoustic Toolbox (2014). <http://oalib.hlsresearch.com/>
- [6] Sakov, P., Counillon, F., Bertino, L., Lisæter, K. A., Oke, P. R., and Korablev, A. (2012). "TOPAZ4: an ocean-sea ice data assimilation system for the North Atlantic and Arctic," *Ocean Sci.*, **8**, 633–656.
- [7] Mellberg, L. E., et al (1991). "Acoustic propagation in the western Greenland Sea frontal zone," *J. Acoust. Soc. Am.* **89**, 2144–56.
- [8] ACOBAR (2014). <http://acobar.nersc.no/>
- [9] Renner, A. H. H., Dumont, D., Beckers, J., Gerland, S., and Haas, C. (2013). "Improved characterization of sea ice using simultaneous aerial photography and sea ice thickness measurements," *Cold Reg. Sci.*, **92**, 37–47.
- [10] Dosso, S. E., Heard, G. J., Vinnis, M. (2002). "Source bearing estimation in the Arctic Ocean using ice-mounted geophones," *J. Acoust. Soc. Am.* **112**, 2721–2734.
- [11] Gavrilov, A. N. and Mikhalevsky, P. N. (2006). "Low-frequency acoustic propagation loss in the Arctic Ocean: Results of the Arctic climate observations using underwater sound experiment," *J. Acoust. Soc. Am.* **119**, 3694–3706.